Explicit Model Following Distributed Control Scheme for Formation Flying of Mini UAVs

QASIM ALI AND SERGIO MONTENEGRO
Chair Aerospace Information Technology, University of Würzburg, Würzburg 97074, Germany

Corresponding author: Q. Ali (qasim.ali@uni-wuerzburg.de)

ABSTRACT A centralized heterogeneous formation flight position control scheme has been formulated using an explicit model following design, based on a Linear Quadratic Regulator Proportional Integral (LQR PI) controller. The leader quadcopter is a stable reference model with desired dynamics whose output is perfectly tracked by the two wingmen quadcopters. The leader itself is controlled through the pole placement control method with desired stability characteristics, while the two followers are controlled through a robust and adaptive LQR PI control method. Selected 3-D formation geometry and static stability are maintained under a number of possible perturbations. With this control scheme, formation geometry may also be switched to any arbitrary shape during flight, provided a suitable collision avoidance mechanism is incorporated. In case of communication loss between the leader and any of the followers, the other follower provides the data, received from the leader, to the affected follower. The stability of the closed-loop system has been analyzed using singular values. The proposed approach for the tightly coupled formation flight of mini unmanned aerial vehicles has been validated with the help of extensive simulations using MATLAB/Simulink, which provided promising results.

INDEX TERMS Distributed control, formation flight, model following, quadcopter, unmanned aerial vehicle.

I. INTRODUCTION

Mini Unmanned Aerial Vehicles (MUAVs) are drawing attention of scientific community from diverse disciplines due to their versatile applications. Their popularity has increased exponentially particularly during the last decade. MUAVs have the advantages over manned platforms with regard to their much lower cost, risk avoidance for human pilots, and their remote sensing capabilities. MUAVs have already replaced manned aircraft in many fields and are even capable to perform novel assignments which cannot be performed by manned platforms. These vehicles are becoming more and more multifaceted as the sensors are miniaturized and on-board computing power is enhanced. Their applications range from simple toys found at electronic supermarkets for entertainment purpose to highly sophisticated commercial platforms performing unusual assignments like offshore wind power station inspection and 3D modeling of buildings [1]. Today MUAVs are a popular research platform serving the humanity in a number of ways like forest fire monitoring, spraying the insecticides, and flood damage assessment etc.

Some other interesting applications are envisaged that may not be performed efficiently by a single MUAV and necessitate the use of multiple units. Such valuable applications include cooperative transportation, fire-fighting, search and rescue, communication relays, and air refueling etc. A group of low-cost UAVs designed for cooperative missions provides redundancy and more effectiveness compared with a single high-tech and expensive UAV. However control requirements are generally more stringent and performance criteria are higher for such applications. More innovative applications are foreseen with advancement in autonomous control techniques.

In order to ensure stability of the formation, robust controllers are mostly proposed to provide insensitivity to possible uncertainties in the motion of other vehicles and communication delays. Adaptive control schemes are used to improve performance and reliability of aerial platforms. These techniques are useful to handle modeling uncertainties and time varying dynamics. As an aerial vehicle is required to operate under different environmental conditions and

performance requirements are also inflexible in case of formation flight; a robust as well as adaptive control scheme is highly desired.

A. RELATED WORK

Different control schemes have been successfully employed for formation flight of aerial vehicles. Some of the contributions are mentioned here. GRASP laboratory at University of Pennsylvania has demonstrated many technological innovations in the domain of autonomous micro UAVs flying inside the constrained environment and performing fantastic feats like cooperatively grasping and transportation [2] using decentralized PID control laws. A solution using Nonlinear Model Predictive Control (NMPC) was proposed in [3] where formation flight of multiple UAVs is sustainable, even in case of communication failure, using relative distance and own motion information. Coordination and trajectory tracking control design for a leader/follower structure of multiple mini rotorcrafts was simulated in [4] using nonlinear coordinated control design with state feedback. H_∞/ℓ_1 control was exploited at Technical University of Hamburg-Harburg (TUHH) for formation flight simulation of multiple quadcopters that guarantees robust stability [5].

Reference [6] combined the tracking control law with an eigenstructure assignment and optimization technique to compute the feedback and feedforward gain matrices, and applied it for pitch pointing control. An important approach to control design is *model following* where it is desired for the quadcopter to perform like an ideal model with desired flying qualities. Pitch pointing flight control laws have been designed in [7] by using the model following control scheme utilizing an eigenstructure assignment and Command Generator Tracker (CGT). In [8], CGT based direct model reference adaptive controller has been exploited to eliminate the adverse effects of bounded uncertainties for Mars atmospheric entry guidance. A leader-follower formation strategy was realized in [9] utilizing a robust tracking control approach; and a Kalman filter based formation command generator was executed on the follower to keep in formation. A cluster of UAVs has been used as a phased array antenna in [10] to show the feasibility of a distributed control strategy. Here each vehicle has a local controller that is based on the information of its own states as well as states of a subset of other vehicles in the formation. A 2D model of quadcopter is considered in this study. In Ref. [11], each quadcopter plans its trajectory based on the information of neighboring quadcopter including its planned trajectory and an estimate of its states. Formation is described by the shape vectors and quadcopters can safely change the shape of formation. Graph theory has been exploited by a number of researchers in the domain of formation control; e.g. using directed graphs [12] and UAV swarm modelling [13] etc. Problem is formulated while converting the graph into Laplacian matrix that gives an insight into the communication topology, and graph connectivity through its eigenvalues. Problem formulation based on graph theory helps to handle communication topology and formation control matters for a large number of units.

Although a number of sophisticated adaptive and robust control schemes have been suggested for formation flight of aerial vehicles, however the algorithms involved are complex from implementation point of view. Each scheme has its own merits and demerits. For e.g., PID controller is non-model based, however the optimality and robustness cannot be guaranteed. H_∞ control is a robust and suboptimal control scheme; however using this design alone it is difficult to obtain a controller with a desired structure [14]. There is generally a trade-off between the intricacy of control technique employed and the level of accuracy achieved there off. Proposed scheme for tightly coupled formation flight combines many advantages of various control schemes including excellent trajectory tracking performance and disturbance rejection, with the additional advantage of simplicity in implementation. Explicit model following design based on LQR PI control scheme also offers the advantage that performance criteria are clearly described for the follower quadcopters to make them behave like the model with desired dynamics. The approach may be used even for some critical flight phases, like automatic flare control for smooth touchdown, where the model dictates the desired trajectory. Implementation of this scheme for *centralized heterogeneous leader follower architecture* is not seen in the literature, as per the knowledge of authors. Also compared with most of the earlier contributions, a full-state vector of quadcopter is considered in this study while tracking only the outputs of interest (performance output) in the presence of perturbations and communication delays. Tracking performance is demonstrated through simulations for a wide range of commands including step, ramp and other varying commands.

II. PROBLEM FORMULATION

MUAVs are classified into fixed wing and rotary wing aircraft (rotorcraft). All rotorcraft have Vertical Take-Off and Landing (VTOL) capability. Quadcopter is the most popular VTOL device due to its agility, ease of construction, and no requirement for a take-off/landing strip. Quadcopter is the focus of our present study and we have chosen *leader-follower* constellation architecture in a *V-shaped* formation as it is more intuitive and inspired by the nature [1]. With this scheme, trajectory of the leader defines the trajectory of the formation. It is desired for the leader to track a commanded signal that may be constant or time-varying. Controller on-board the leader is designed to keep the output values close to the commanded values. For the formation, the states of the leader constitute the coordination variable, since the actions of the other vehicles in the formation are completely specified once the leader states are known [15]. Each follower's control is designed to maintain its user-defined position in formation using the information of its own states and the leader states. Information of leader may be received either via inter-vehicle communication or estimated using the sensors (e.g. radar, laser scanner, PMD camera etc.)

onboard the followers. We here assume that information of leader is always available to the followers. It may be through communication link, or sensors onboard the followers, or received via the other follower. Communication topology of leader and two followers for this study is shown in Fig. 1. In case of communication loss between leader and any of the followers, the other follower quadcopter provides the leader's states to affected follower quadcopter in order to keep the formation intact.
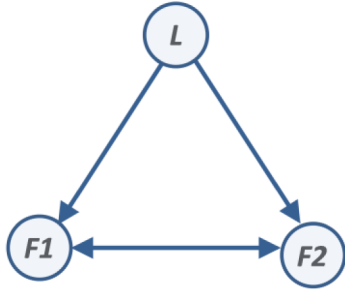

FIGURE 1. Communication topology of quadcopters in formation.

A. QUADCOPTER DYNAMIC MODEL

Quadcopter motion dynamics are described in a number of publications e.g. [16]. However these are described here for completeness. Quadcopter has four rotors numbered 1 – 4, as shown in Fig. 2, representing front, left, rear, and right rotors respectively. Front and rear rotors rotate anti-clockwise while left and right rotors rotate clockwise. Thus two pairs of rotors mutually cancel the gyroscopic effects and aerodynamic torques. Unlike a fixed-wing aircraft with conventional control surfaces, a quadcopter is controlled through differential speed of rotors. In hovering mode, speeds of all four rotors are same. Vertical motion is controlled through aggregate thrust generated by all rotors. Pitch angle (around y-axis) is generated through differential speeds of front and rear rotors causing the forward/backward motion in x-direction.
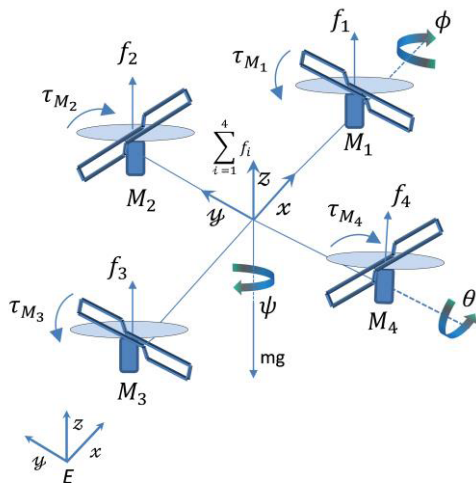

FIGURE 2. Quadcopter motion dynamics.

Similarly for lateral motion in y-direction, speeds of left and right rotors are varied differentially thereby generating the roll angle and corresponding motion. For yawing motion, speeds of pair of rotors 1 & 3 are varied compared with 2 & 4 in such a manner that total thrust remains same in order to maintain the altitude. Torque so generated causes the yaw motion. Thus all rotors play their role for yaw motion.

Quadcopter dynamics, as described above, are modeled as per the following equations [17]:

$$\begin{aligned}
u &= f_1 + f_2 + f_3 + f_4 \\
f_i &= k_i \omega_i^2, \quad i = 1 \dots 4 \\
m\ddot{x} &= -u \sin\theta \\
m\ddot{y} &= u \cos\theta \sin\phi \\
m\ddot{z} &= u \cos\theta \cos\phi - mg \\
\ddot{\psi} &= \tau_\psi \\
\ddot{\theta} &= \tau_\theta \\
\ddot{\phi} &= \tau_\phi
\end{aligned} \tag{1}$$

Here u shows the total thrust generated by four rotors, f_i is the force produced due to the rotation of rotor i, $k_i > 0$ is a constant, ω_i is the angular speed of motor i (M_i, $i = 1 \dots 4$), m is mass of quadcopter, and g is gravitational constant. τ_ψ, τ_θ and τ_ϕ represent the control inputs for yawing, pitching, and rolling moments respectively.

Quadcopter system under consideration has four inputs, twelve states, and six outputs. Our state vector comprises $[x\ \dot{x}\ y\ \dot{y}\ z\ \dot{z}\ \psi\ \dot{\psi}\ \theta\ \dot{\theta}\ \phi\ \dot{\phi}]$. It represents the 3D position of center of mass of quadcopter in x, y and z-direction relative to the earth-fixed frame E [17], and Euler angles namely the yaw angle (ψ) around the z-axis, the pitch angle (θ) around the y-axis, and the roll angle (ϕ) around the x-axis respectively with their time derivatives denoted with dot (.) overhead. Output vector is $[x\ y\ z\ \psi\ \theta\ \phi]$, and performance output vector is $[x\ y\ z]$.

Now we define the following state equations in order to linearize the system (1) as given in [18]:

$$\begin{aligned}
\zeta &= [x_1\ x_2\ x_3\ x_4\ x_5\ x_6\ x_7\ x_8\ x_9\ x_{10}\ x_{11}\ x_{12}]^T \\
&= [x\ \dot{x}\ y\ \dot{y}\ z\ \dot{z}\ \psi\ \dot{\psi}\ \theta\ \dot{\theta}\ \phi\ \dot{\phi}]^T
\end{aligned}$$

Our control vector is

$$U = [u_1\ u_2\ u_3\ u_4]^T = [u - mg\ \tau_\psi\ \tau_\theta\ \tau_\phi]^T$$

Dynamic equations may be written as

$$\begin{bmatrix} \dot{x}_1 \\ \dot{x}_2 \\ \dot{x}_3 \\ \dot{x}_4 \\ \dot{x}_5 \\ \dot{x}_6 \\ \dot{x}_7 \\ \dot{x}_8 \\ \dot{x}_9 \\ \dot{x}_{10} \\ \dot{x}_{11} \\ \dot{x}_{12} \end{bmatrix} = \begin{bmatrix} x_2 \\ -u_1 \sin x_9 / m - g\sin x_9 \\ x_4 \\ u_1 \cos x_9 \sin x_{11} / m + g\cos x_9 \sin x_{11} \\ x_6 \\ u_1 \cos x_9 \cos x_{11} / m + g\cos x_9 \cos x_{11} - g \\ x_8 \\ u_2 \\ x_{10} \\ u_3 \\ x_{12} \\ u_4 \end{bmatrix}$$

or shortly:

$$\dot{\zeta} = f(\zeta, \mho)$$

Now let $\zeta = 0$ be an equilibrium point with $f(0,0) = 0$. The linearization by Taylor series about the origin gives the following linear system

$$\dot{\zeta} = A\zeta + B\mho \qquad (2)$$

Where A and B represent the state matrix and input matrix respectively. For further details, please refer to [18]. Longitudinal and lateral dynamics are decoupled after linearization. Instead of focusing on either lateral or longitudinal dynamics, we consider them simultaneously. Leader dynamic model is taken as a reference model thereby defining the ideal output response to be followed by two wingmen. We further assume a *heterogeneous formation* i.e. the leader hardware (and hence mass) is different from the followers to simulate a more realistic scenario. This assumption is based on the fact that in reality a leader is likely to be more equipped than followers in terms of sensors and hence will be more massive. Ref. [19] defines *micro UAVs* that are between $0.1 - 0.5$ kg. For our present study, we have assumed that the mass of leader is 2 kg and that of followers is 0.64 kg each, hence new acronym of MUAV has been introduced in this paper to refer to *mini UAVs*.

B. FORMATION DYNAMIC MODEL

Desired dynamics of the leader, referred to as reference model, are defined as a Linear Time-Invariant (LTI) system in the form:

$$\dot{X}_L = A_L X_L + B_L r(t)$$
$$Y_L = C_L X_L + D_L r(t) \qquad (3)$$

Suffix L represents the leader and F will represent follower. For the system (3), $X_L \epsilon R^{n_L}$ are states of the leader quadcopter, $r(t)$ is the external bounded command value, and $Y_L \epsilon R^{p_L}$ is the performance output vector of leader. Leader state space matrices (A_L, B_L, C_L, D_L) have their conventional meaning. For the leader to exhibit stable dynamics, the state matrix A_L of the leader needs to be *Hurwitz* i.e. all its eigenvalues should have strictly negative real part.

Follower quadcopter dynamics are described as follows:

$$\dot{X}_F = A_F X_F + B_F \mho$$
$$Y_F = C_F X_F + D_F \mho \qquad (4)$$

Here $X_F \epsilon R^{n_F}$ are states of the follower quadcopter, $\mho \epsilon R^{m_F}$ is the control vector, and $Y_F \epsilon R^{p_F}$ is the performance output vector of follower with $p_F \leq m_F$ [20]. p_F and m_F refer to number of outputs Y_F and number of control inputs $\mho$ respectively. The matrices (A_F, B_F, C_F, D_F) are of corresponding dimensions. Quadcopter is an under-actuated system (four inputs and 6DOF motion) and Linear Quadratic Regulator Proportional Integral (LQR PI) approach is not applicable for under-actuated systems [14] to track all outputs. However this control scheme may be applied with suitable formulation of problem while tracking only the outputs of interest (performance output). With this scheme, maximum number of trackable outputs may not exceed number of control inputs (four in case of quadcopter). It is assumed that the matrix pair (A_F, B_F) is stabilizable and state vectors X_L and X_F are available as these are to be used for formulation of control signal $\mho$ for follower.

Before implementing the controller, we first do the controllability check for the followers using the controllability matrix $P = [B_F \ A_F \ B_F \ A_F^2 \ B_F \ldots A_F^{n_f - 1} B_F]$ and find it to be full ranked. All the closed-loop poles of the leader may be assigned to desired locations through pole placement method. Though leader in our study is controlled through pole placement method, however same may be controlled though some other scheme as well e.g. LQR. Leader receives a known bounded command $r(t)$ that may or may not vary with time. It is emphasized that the proposed control scheme is meant for the followers to maintain the desired separations from the leader. For *centralized* leader-follower architecture, we are primarily interested to determine $\mho$ for the follower such that the desired 3D formation geometry, given by the relative distance vector $r = [r_x \ r_y \ r_z]^T$, is maintained. For this an LQR controller with PI feedback connection [20] is implemented for the follower. We assume that all the states of quadcopters are available through suitable sensors. The control signal is computed with LQR scheme while suitably augmenting the states of follower with that of leader. Design objectives in LQR scheme are defined through Q and R matrices. Q matrix, a positive semi-definite matrix, shows the weightage (or importance) to states. R being a positive definite matrix indicates weightage of control efforts corresponding to control inputs. The controller can be tuned by changing the elements in the Q and R matrices to achieve a desirable response. An efficient LQR control scheme is based on finding the right weighting factors. Q and R matrices used for this study are given in the Appendix.

Model following LQR PI control scheme given in [20] has been exploited for our present study and tailored for leader-follower tightly coupled formation flight. Open-loop dynamics of follower and leader may be formulated as:

$$\begin{bmatrix} \dot{X}_F \\ \dot{X}_L \end{bmatrix} = \begin{bmatrix} A_F & O_{n_F \times n_L} \\ O_{n_L \times n_F} & A_L \end{bmatrix} \begin{bmatrix} X_F \\ X_L \end{bmatrix} + \begin{bmatrix} B_F \\ O_{n_L \times m_F} \end{bmatrix} \mho + \begin{bmatrix} O_{n_F \times m_F} \\ B_L \end{bmatrix} r(t) \qquad (5)$$

Tracking error represented as ΔY may be written as:

$$\Delta Y = Y_F - Y_L = C_F X_F + D_F \mho - C_L X_L - D_L r(t) \quad (6)$$

Writing (6) in matrix form:

$$\Delta Y = \begin{bmatrix} C_F & -C_L \end{bmatrix} \begin{bmatrix} X_F \\ X_L \end{bmatrix} + D_F \mho + (-D_L) r(t) \qquad (7)$$

Now the open-loop dynamics given by (5) and (7) may be written concisely as:

$$\dot{X} = A X + B \, Ʉ + B_r \, r(t)$$

$$\Delta Y = C X + D \, Ʉ + D_r \, r(t) \tag{8}$$

We aim to find such a Ʉ that the tracking error (or system output) asymptotically tends to zero in the presence of any known, bounded, and possibly time varying command $r(t)$. Formulation of above problem suggests that the tracking problem has been converted into a regulation problem [21], referred to as CGT. Now an *Integral Control* is applied to track a step input command with zero errors. For this scenario a practical tracker like CGT is chosen. Integrated tracking error $\dot{e}_y$ may be written as:

$$\dot{e}_y = \Delta Y \tag{9}$$

Introducing (9) into system dynamics (8), it gives

$$\begin{bmatrix} \dot{e}_y \\ \dot{X} \end{bmatrix} = \begin{bmatrix} O_{pF \times pF} & C \\ O_{(n_F + n_L) \times pF} & A \end{bmatrix} \begin{bmatrix} e_y \\ X \end{bmatrix} + \begin{bmatrix} D \\ B \end{bmatrix} Ʉ$$
$$+ \begin{bmatrix} D_r \\ B_r \end{bmatrix} r(t) \tag{10}$$

Tracking error ΔY may be defined as:

$$\Delta Y = \begin{bmatrix} O_{pF \times pF} & C \end{bmatrix} \begin{bmatrix} e_y \\ X \end{bmatrix} + D \, Ʉ + D_r \, r(t) \tag{11}$$

Equations (10) and (11) may now be written as:

$$\dot{\tilde{X}} = \tilde{A} \tilde{X} + \tilde{B} \, Ʉ + \tilde{B}_r \, r(t)$$

$$\Delta Y = \tilde{C} \tilde{X} + \tilde{D} \, Ʉ + \tilde{D}_r \, r(t) \tag{12}$$

Care is to be exercised while formulating the $\tilde{A}$ matrix for proper dimensions. Also note that for above system (12), total number of states is equal to the sum of vector length of $\Delta Y + X_F + X_L$.

C. CONTROL STRATEGY
Now assuming that external command is step-input command with zero errors then differentiating state dynamics equation of system (12) w.r.t. time and introducing new variables $ɯ = \begin{bmatrix} \dot{e}_y & \dot{X} \end{bmatrix}^T$ and $v = \dot{Ʉ}$, we may write:

$$\dot{ɯ} = \tilde{A} ɯ + \tilde{B} v \tag{13}$$

Open-loop dynamics of (13) may be controlled through LQR control scheme. LQR is a very attractive control approach as it is capable to handle multiple actuators and complex system dynamics. Furthermore, it offers very large stability margins to errors in the loop gain. However, LQR assumes access to the states.

In order to minimize the LQR cost, control input v is used. Cost function J may be defined as:

$$J = \int_0^\infty \left(ɯ^T Q ɯ + v^T R v \right) dt \tag{14}$$

Q and R are LQR weight matrices defined as before. Now solving the Algebraic Riccati Equation (ARE):

$$\tilde{A}^T P + P \tilde{A} + Q - P \tilde{B} R^{-1} \tilde{B}^T P = 0 \tag{15}$$

gives the solution $P = P^T > 0$, that is used to compute the control signal. LQR gain matrix K is given as under:

$$K = R^{-1} \tilde{B}^T P \tag{16}$$

LQR control signal may be written as:

$$v = \dot{Ʉ} = -K \, ɯ \tag{17}$$

LQR PI controller for a MIMO system corresponds to a gain matrix with order equal to the number of elements in $Ʉ \times (\Delta Y + X_F + X_L)$. Our gain matrix is of the following form:

$$K = [K_I^e \; K_p^{X_F} \; K_p^{X_L}] \tag{18}$$

Here subscript indicates the type of gain (proportional or integral) and superscript shows the variable to whom this gain matrix is applied. Now

$$\dot{Ʉ} = -[K_I^e \; K_p^{X_F} \; K_p^{X_L}] \begin{bmatrix} \dot{e}_y \\ \dot{X} \end{bmatrix} \tag{19}$$

or

$$\dot{Ʉ} = -[K_I^e \; K_p^{X_F} \; K_p^{X_L}] \begin{bmatrix} \dot{e}_y \\ \dot{X}_F \\ \dot{X}_L \end{bmatrix} \tag{20}$$

Integrating (20) and ignoring constants of integration, LQR PI control solution for the follower is given as:

$$Ʉ = K_I^e \frac{(Y_L - Y_F)}{s} - K_p^{X_F} X_F - K_p^{X_L} X_L \tag{21}$$

We note that structure of LQR PI gain matrix comprises three parts; a state feedback $K_p^{X_F}$, a feed-forward compensator $K_p^{X_L}$, and an additional feed-forward filter K_I^e in the error channel that guarantees perfect tracking. Although our derivation is based on step reference command, the resulting control system gives good time response for any arbitrary reference command signal $r(t)$ [14], as will be demonstrated in simulation section. Fig. 3 shows the interconnection diagram for LQR PI control scheme implemented for leader-follower architecture. For the sake of brevity, only one follower is shown here. Dynamics of leader and follower plants are defined by (3) and (4) respectively.
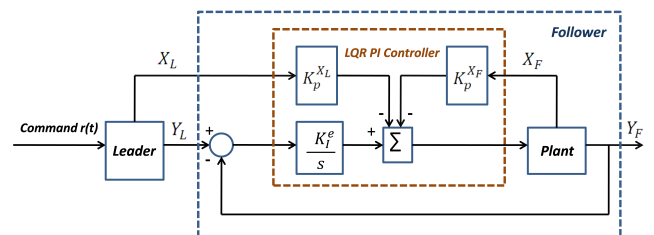

FIGURE 3. LQR PI control scheme for leader-follower architecture.

It is established in [22] that for perfect tracking it is necessary to have as many control inputs in vector Ụ(t) as there are in command signals $r(t)$ for tracking. However we slightly modify it to state that the number of control inputs should be equal to or more than the command signals, as demonstrated in this paper while using three command signals (for 3D position control) and four control signals. We now give some propositions/definitions to determine the stability of a leader-follower architecture based on LQR PI control scheme.

Proposition 1: All signals for a leader-follower formation, based on LQR PI control scheme, are bounded if $\|G_L\|_\infty \le \Gamma$ and $\|K\|_\infty \le \delta$ where G_L is the leader state space model, K is LQR PI gain matrix, and Γ and δ are bounded numbers. Infinity norm of gain matrix K gives an indication of maximum control effort.

Proposition 2: A leader-follower formation based on LQR PI control scheme is stable if $\| \tilde{G}_{cl} \|_\infty \le 1$ where $\tilde{G}_{cl}$ represents the state space system comprising leader-follower, controlled though LQR PI control scheme, and is given by the matrices $(\tilde{A}_{cl}, \tilde{B}, \tilde{C}, \tilde{D})$ where $\tilde{A}_{cl} = \tilde{A} - \tilde{B} * K$.

Definition 1: A leader-follower formation based on LQR PI control scheme is stable if all poles of the matrix $\tilde{A}_{cl}$ are strictly in open left-half plane.

III. SIMULATION RESULTS AND ANALYSIS

From safety point of view, most of the proposed algorithms require to be simulated before actual flights may be undertaken. It also helps to authenticate the efficacy of the algorithm. Above defined model of leader-follower scheme was implemented in MATLAB/Simulink. For this study, possible perturbations on outputs of leader, on control inputs and outputs of followers have been considered and implemented. Wind gust was simulated as a step function on quadcopters outputs. Communication delays between all three agents were also implemented in our simulation model to mimic the real scenarios. System was also tested for step, ramp and sinusoidal commanded values. This command generator is capable of handling a wide range of motion trajectories, including position unit step commands, unit ramp commands, oscillatory commands, and more [23]. Table 1 shows some of the metadata under which the system was simulated while taking a combination of different entries from the table.

Simulation results are depicted in Fig. 4 and Fig. 5 that show the positions of all three units in three-axes and the 3D view of the whole formation respectively in presence of perturbations. Initial and final positions of units are also marked in Fig. 5 to indicate the direction of movement. From the plots, it is evident that output of leader is tracked quite smoothly by the followers while maintaining the desired separations. Another remarkable feature of this scheme is that when some disturbance is encountered on the output of leader (for example a wind gust) and there is some deviation from the intended trajectory, the followers also make the similar movement in order to maintain the formation geometry. Simulations in Fig. 4 and Fig. 5 under different perturbations

TABLE 1. Metadata for simulation.

	Leader	Follower 1	Follower 2	Activation Time (s)
Initial Position	[10,10,10]	[0,2,3]	[4,1,2]	[0,0,0]
Commanded Position	[40,y_des[a],40] & [100,y_des[a],100]	x = -10[b] y = -15[b] z = -5[b]	x = -15[b] y = -10[b] z = -10[b]	[0,0,0]
New Formation Geometry	[40,y_des[a],40]	x = -20[b] y = -30[b] z = -10[b]	x = -30[b] y = -20[b] z = -20[b]	[30,30,30]
Input Disturbance	Nil	[1,1,1,1]	[2,2,2,2]	[20,20,20,20] & [50,50,50,50]
Output Disturbance (wing gust)	[0,0,0]	[5,10,12]	[10,5,15]	[50,60,70] & [40,50,60]
Comm. Delay	[1,1][c]	[1,1][d]	[2,2][e]	-
Comm. Loss	-	-	-	35[f]

[a]*y_des* is a ramp command with slope 1 for changing position in y-direction.
[b]Separation between leader and follower.
[c]For states & outputs between leader and follower 1.
[d]For states & outputs between leader and follower 2.
[e]For states & outputs between follower1 and follower 2.
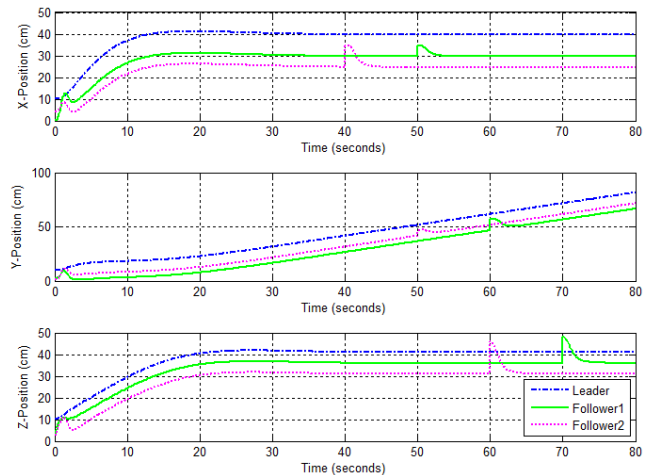[f]Communication loss between leader and follower 1.

FIGURE 4. Three-axes position of whole formation under disturbances.

at different time instants show excellent tracking performance for commanded values in the form of step inputs (x-axis and z-axis) and ramp command (y-axis).

For a formation having a single leader, the equilibrium point is the desired relative position of the vehicles [24] that is shown to be maintained under a number of perturbations as depicted in Fig. 4 and Fig. 5. Results may also be interpreted as follower quadcopters exhibiting the *static stability*. This was verified by observing their immediate response following a disturbance from a trimmed flight condition [14], where follower quadcopters returned to their equilibrium points.

Contrary to the Proportional Differential (PD) approach used in [18], no oscillation behavior is observed in steady state with the use of LQR PI control scheme that shows its strength. One PID controller gives one control signal at a time. However for controllers like LQR, all the states are
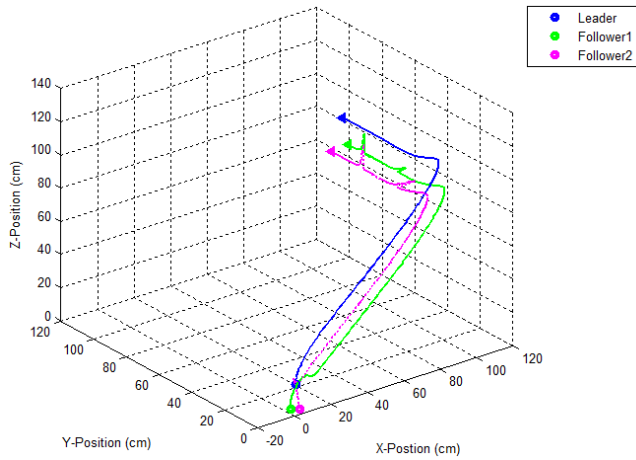
FIGURE 5. Trajectory for leader and followers under disturbances.

taken care of simultaneously with the use of controller in the form of matrix K that facilitates to provide multiple appropriate control signals at the same time. Solving matrix equations allows all the control gains to be computed simultaneously so that all loops are closed at the same time [14].

Some missions may require to change the formation geometry during flight to cope with changing situations and environment, like collision avoidance. In order to simulate such scenario, we changed the formation geometry at $t = 30s$ while doubling the separations between leader and followers. Corresponding simulation is shown in Fig. 6 that reveals excellent performance to maintain new desired formation geometry even under perturbations at different time instants. For this particular maneuver and formation geometry, separations are increased among all the units so collisions are not imagined. However for a different scenario, a suitable collision avoidance scheme is required to be adopted.
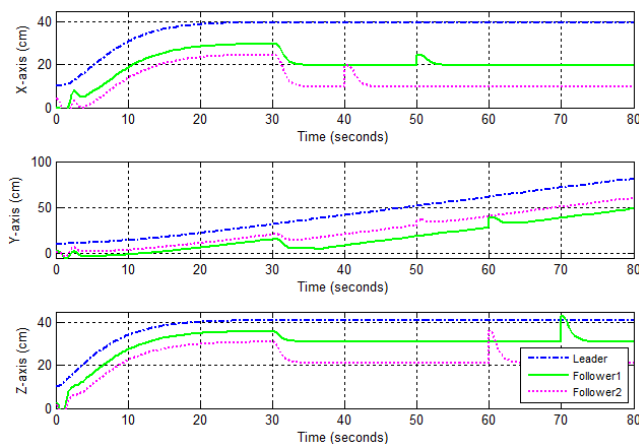

FIGURE 6. Three axes position of MUAVs under switching formation geometry.

We now incorporate all the possible perturbations with their numerical values depicted in Table 1 and plot the relative distances between all the three units while also changing the

formation geometry at $t = 30s$. Corresponding plot is shown in Fig. 7 which demonstrates that required *3D* formation geometry is maintained under a number of disturbances.
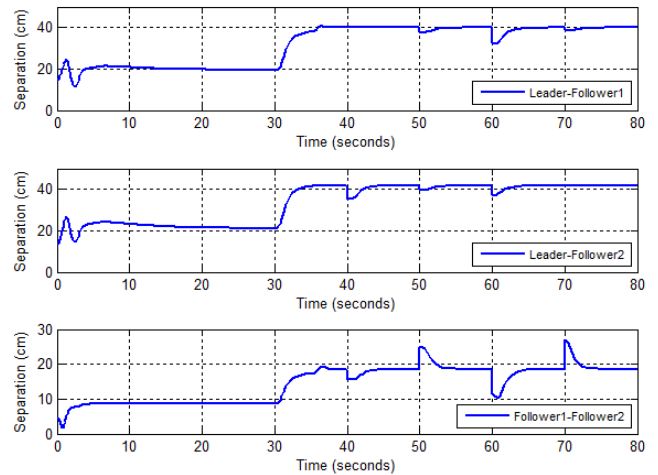

FIGURE 7. Inter-unit separations in the formation.

Now we show the response of whole formation for a sinusoidal command to the leader on X-axis with a frequency of 0.3 rad/sec and a bias of 40cm. Plot to this effect, in the presence of disturbances, is shown in Fig. 8. However for such commands, desired tracking (of same frequency) is achieved if rate of change of command signal is within the closed-loop system bandwidth [20]. Though we get the sinusoidal output but with a different amplitude and phase determined by the magnitude of the system transfer function. Desired amplitude may be achieved using a suitable pre-compensator. Thus the control scheme is capable of tracking varying set-points as well.
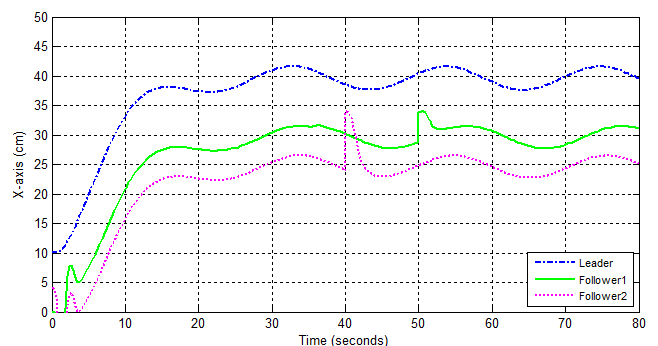

FIGURE 8. Response of formation under a sinusoidal command.

Quadcopters trajectories in all the foregone plots are shown for about one meter only to clearly show the effects of perturbations and their rejection. We now show the formation trajectory under time-varying command for a distance of 20m, 1m and 12m in X-, Y- and Z-direction respectively in Fig. 9.

In order to further verify the health of simulation results, we now introduce a perturbation of magnitude [10,5,15] on
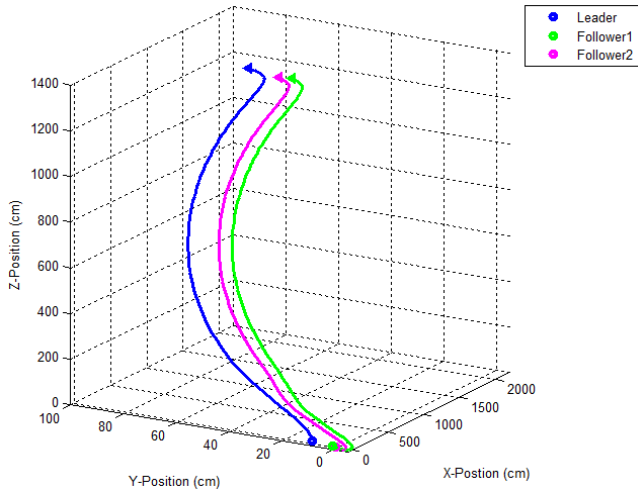
FIGURE 9. Trajectory of formation for an extended distance.

follower2 on X-, Y-, and Z-axis individually at $t = 40, 50$, and 60 seconds respectively. Required throttle input and control inputs for the yawing, pitching and rolling moments [17] to bring the quadcopter back to desired equilibrium condition are shown in Fig. 10 that gives the expected results. This plot is just to realize how the control inputs are exercised to cater for the perturbations on the desired position.
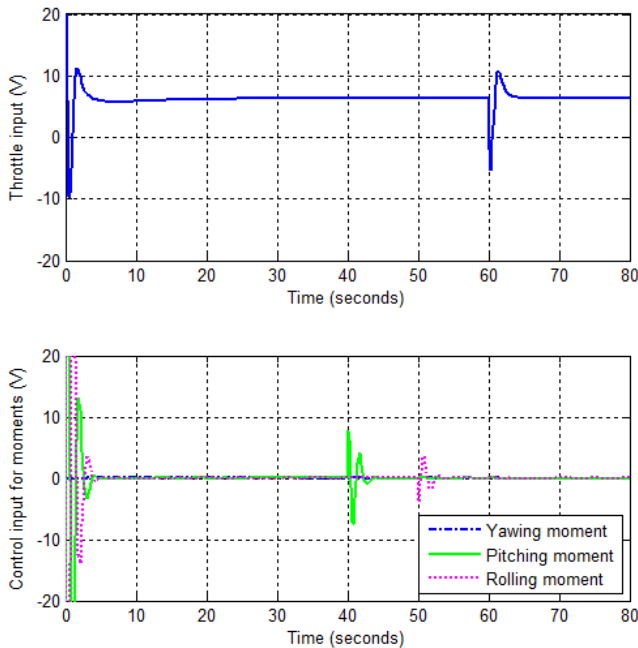

FIGURE 10. Control input for throttle and moments to regain equilibrium.

Pulse Width Modulation (PWM) output values of four motors speed are as following, as defined in [18]:

$$PWM_{M1} = u + \tau_\theta + \tau_\psi$$
$$PWM_{M2} = u - \tau_\phi - \tau_\psi$$
$$PWM_{M3} = u - \tau_\theta + \tau_\psi \qquad (22)$$
$$PWM_{M4} = u + \tau_\phi - \tau_\psi$$

Control voltages of four motors (under the same perturbations and time instants) to bring the quadcopter back to its desired position are plotted in Fig. 11 that are commensurate with the expected results.
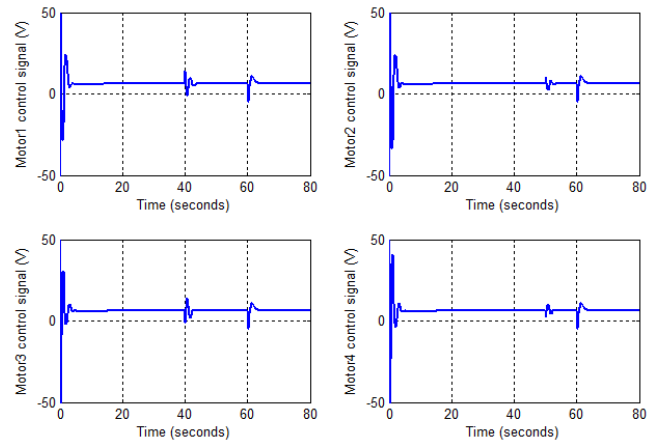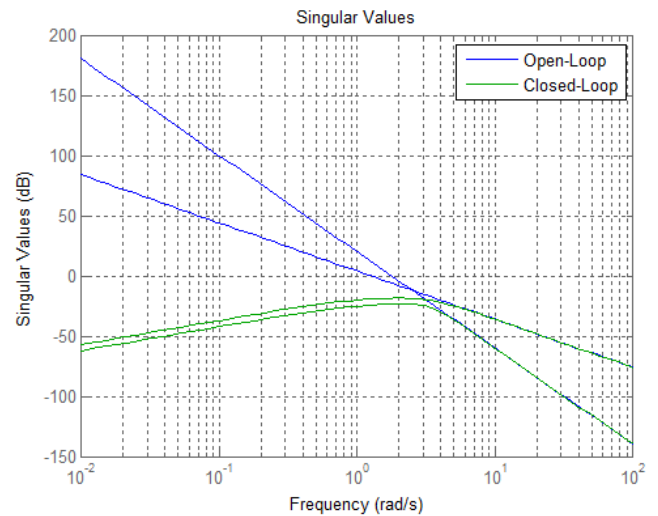

FIGURE 11. Control voltages of four motors of quadrocopter.

FIGURE 12. Sigma plot for leader-follower scheme in open-loop and closed-loop.

A. STABILITY ANALYSIS

For a MIMO system, individual gain and phase margins between different pairs of inputs and outputs mean little from the point of view of overall robustness [14]. This is due to the coupling that generally exists between different inputs and outputs of a MIMO system. Singular values are useful for robustness analysis of a MIMO system. Singular values can provide a better indication of the overall response, stability, and conditioning of a MIMO system than a channel-by-channel Bode plot. Sigma plot also gives indication of crossover frequency. At this frequency we get the same output frequency as commanded value, though output amplitude will be different determined by transfer function of the system. In MATLAB, we can get it through the command *getGainCrossover (sys, gain)*. H_∞ norm of a MIMO system is the

largest singular value across frequencies and hence is an indicator of stability of a MIMO system. Sigma plot of $\tilde{G}$ and $\tilde{G}_{cl}$ representing leader-follower system in open-loop and closed-loop respectively are shown in Fig. 12 which demonstrates that LQR PI control scheme has efficiently controlled the system. The maximum singular value (-18.4 dB) for the closed-loop system is below an upper limit (0 dB) that guarantees stability despite parameter variations in the linearized model. This maximum singular value corresponds to H_∞ norm of 0.12 thereby providing sufficient gain margin. At low frequencies also, singular values of closed-loop system are below 0 dB, unlike open-loop system where these are much higher than the threshold value.

IV. CONCLUSION AND FUTURE WORK

For centralized formation flying we are interested for followers to track varying output of leader in order to smoothly maintain relative *3D* distances. For presented algorithm, extensive simulations were realized under a number and types of disturbances including input disturbance on control values, output disturbances (e.g. a wind gust) and communication delays. It revealed the follower systems to be quite robust in terms of maintaining the desired formation geometry. This technique has promising results in terms of stability and leader output tracking even in the presence of significant perturbations and under arbitrary switching formation geometries during flight. The approach is appropriate for the scenarios where tightly coupled formation flight is desired like cooperative grasping, joint load transportation etc.

Proposed approach for followers in the formation, is simple from implementation point of view. However it necessitates to know the exact dynamic model of aerial vehicles. It also assumes that states of leader and followers are available. In case of non-availability of states, a suitable *observer* may be designed for estimation of states. Although this scheme is suitable for small formations, however appropriate arrangements may be made to extend it to medium sized formations.

As it is quite laborious to model all the dynamics of rotorcraft flying in close formation, adaptive and robust control techniques, like LQR PI, may be explored to their full potential to cater for such scenarios. For future work, presented scheme may be implemented in real-time using the formation flying test setup developed at Institute of Aerospace Information Technology, Würzburg University [25]. A suitable collision avoidance mechanism may also be implemented for safe operations.

APPENDIX

Desired poles for leader

$= [-1.9054 + 1.6368i, -1.9054 - 1.6368i, -0.2350 + 0.0835i, -0.2350 - 0.0835i, -0.1737 + 0.0720i, -0.1737 - 0.0720i, -1.9054 + 1.6368i, -1.9054 - 1.6368i, -0.2350 + 0.0835i, -0.2350 - 0.0835i, -3.1214 + 0.0000i, -0.5065 + 0.0000i];$

Gain matrix for leader using pole placement

$= [0.0557, 0.1602, 0.1641, 0.4351, 0.5483, 2.5271, 0.3093, 1.9635, 0.6765, -0.2422, -0.2322, 0.1653; -0.0172, 0.4065, 0.1405, 0.3571, 0.3443, 1.1077, 0.4117, 2.4180, -1.3149, -0.4698, -0.2773, 0.1314; -0.0381, -0.3742, -0.0096, -0.0279, -0.0248, -0.0458, -0.0387, -0.1789, 8.4567, 4.4017, -0.1616, -0.1089; 0.0008, 0.0591, 0.0559, 0.3689, 0.0445, 0.1450, 0.0472, 0.2508, -0.3756, -0.1682, 8.4043, 4.4536]$

Q matrix (for LQR PI)

$= \text{diag}([4000, 4000, 5000, 4000, 1, 4000, 1, 5000, 20, 0.25, 1, 1000, 50, 1000, 50, 4000, 1, 4000, 1, 5000, 20, 0.25, 1, 1000, 50, 1000, 50]);$

R matrix (for LQR PI) $= \text{diag}([100, 0.1, 25, 25]);$

REFERENCES

[1] Q. Ali, N. Gageik, and S. Montenegro, "A review on distributed control of cooperating mini UAVs," *Int. J. Artif. Intell. Appl.*, vol. 5, no. 4, pp. 1–13, Jul. 2014. [Online]. Available: http://airccse.org/journal/ijaia/papers/5414ijaia01.pdf

[2] D. Mellinger, M. Shomin, N. Michael, and V. Kumar, "Cooperative grasping and transport using multiple quadrotors," in *Distributed Autonomous Robotic Systems*. Berlin, Germany: Springer, 2013, pp. 545–558.

[3] H.-S. Shin, M.-J. Thak, and H.-J. Kim, "Nonlinear model predictive control for multiple UAVs formation using passive sensing," *Int. J. Aeronautical Space Sci.*, vol. 12, no. 1, pp. 16–23, 2011. [Online]. Available: http://central.oak.go.kr/repository/journal/10521/HGJHC0_2011_v12n1_16.pdf

[4] J. A. Guerrero, I. Fantoni, S. Salazar, and R. Lozano, "Flight formation of multiple mini rotorcraft via coordination control," in *Proc. ICRA*, May 2010, pp. 620–625.

[5] U. Pilz and H. Werner, "An $\mathcal{H}_\infty/\ell_1$ approach to cooperative control of multi-agent systems," in *Proc. 51st CDC*, Dec. 2012, pp. 5930–5935.

[6] D. Kim and Y. Kim, "Optimized feedforward design scheme unifying regulator and command generator tracker," *J. Guid., Control, Dyn.*, vol. 19, no. 4, pp. 899–904, 1996. [Online]. Available: http://arc.aiaa.org/doi/pdf/10.2514/3.21716

[7] K. M. Sobel and E. Y. Shapiro, "A design methodology for pitch pointing flight control systems," *J. Guid., Control, Dyn.*, vol. 8, no. 2, pp. 181–187, 1985. [Online]. Available: http://arc.aiaa.org/doi/pdf/10.2514/3.19957

[8] S. Li and Y. Peng, "Command generator tracker based direct model reference adaptive tracking guidance for Mars atmospheric entry," *Adv. Space Res.*, vol. 49, no. 1, pp. 49–63, 2012.

[9] B. Wang, X. Dong, B. M. Chen, T. H. Lee, and S. K. Phang, "Formation flight of unmanned rotorcraft based on robust and perfect tracking approach," in *Proc. ACC*, Jun. 2012, pp. 3284–3290.

[10] S. Tonetti, M. Hehn, S. Lupashin, and R. D'Andrea, "Distributed control of antenna array with formation of UAVs," in *Proc. 18th IFAC World Congr.*, 2011, pp. 7848–7853.

[11] M. Turpin, N. Michael, and V. Kumar, "Decentralized formation control with variable shapes for aerial robots," in *Proc. ICRA*, May 2012, pp. 23–30.

[12] A. P. Popov and H. Werner, "A robust control approach to formation control," in *Proc. ECC*, Aug. 2009, pp. 4428–4433.

[13] A. Chapman and M. Mesbahi, "UAV swarms: Models and effective interfaces," in *Handbook of Unmanned Aerial Vehicles*. Dordrecht, The Netherlands: Springer, 2014, pp. 1987–2019.

[14] B. L. Stevens and F. L. Lewis, *Aircraft Control and Simulation*. New York, NY, USA: Wiley, 2003.

[15] W. Ren, R. W. Beard, and T. W. McLain, "Coordination variables and consensus building in multiple vehicle systems," in *Cooperative Control*. Berlin, Germany: Springer, 2005, pp. 171–188.

[16] M. I. Rashid and S. Akhtar, "Adaptive control of a quadrotor with unknown model parameters," in *Proc. 9th IBCAST*, Jan. 2012, pp. 8–14.

[17] P. Castillo, A. Dzul, and R. Lozano, "Real-time stabilization and tracking of a four-rotor mini rotorcraft," *IEEE Trans. Control Syst. Technol.*, vol. 12, no. 4, pp. 510–516, Jul. 2004.

[18] D. Lara, A. Sanchez, R. Lozano, and P. Castillo, "Real-time embedded control system for VTOL aircrafts: Application to stabilize a quad-rotor helicopter," in *Proc. CCA*, Munich, Germany, Oct. 2006, pp. 2553–2558.

[19] V. Kumar and N. Michael, "Opportunities and challenges with autonomous micro aerial vehicles," *Int. J. Robot. Res.*, vol. 31, no. 11, pp. 1279–1291, 2012. [Online]. Available: http://ijr.sagepub.com/content/31/11/1279.full.pdf

[20] E. Lavretsky, "Robust and adaptive control methods for aerial vehicles," in *Handbook of Unmanned Aerial Vehicles*. Dordrecht, The Netherlands: Springer, 2015, pp. 675–710.

[21] G. F. Franklin, J. Da Powell, and A. Emami-Naeini, *Feedback Control of Dynamic Systems*. Reading, MA, USA: Addison-Wesley, 1988.

[22] H. Kwakernaak and R. Sivan, *Linear Optimal Control Systems*. New York, NY, USA: Wiley, 1972.

[23] F. L. Lewis, H. Zhang, K. Hengster-Movric, and A. Das, *Cooperative Control of Multi-Agent Systems: Optimal and Adaptive Design Approaches*. London, U.K.: Springer, 2013.

[24] J. A. Fax and R. M. Murray, "Information flow and cooperative control of vehicle formations," *IEEE Trans. Autom. Control*, vol. 49, no. 9, pp. 1465–1476, Sep. 2004.

[25] Q. Ali and S. Montenegro, "A simple approach to quadrocopter formation flying test setup for education and development," in *Proc. 9th INTED*, Madrid, Spain, 2015, pp. 2776–2784.

QASIM ALI received the B.E. degree in avionics engineering from the National University of Sciences and Technology (NUST), Islamabad, in 1999, and the M.S. degree in control systems from Air University, Islamabad, in 2010. He is currently pursuing the Ph.D. degree in navigation, guidance, and control with the University of Würzburg, Germany. His research interests include GNSS-based precise positioning, flight simulations, and navigation, guidance, and control in the domain of mini unmanned aerial vehicles.

Mr. Ali received the Gold Medal for his M.S. degree. He is a recipient of the HEC/DAAD Scholarship for his Ph.D. studies in Germany.

SERGIO MONTENEGRO received the B.S. degree from the Universidad del Valle, in 1982, and the M.S. and Ph.D. degrees in computer science from the Technical University of Berlin, in 1985 and 1989, respectively.

He was a Research Assistant in Distributed Computing with the Fraunhofer-Gesellschaft Institut, Berlin, from 1985 to 2007. From 2007 to 2010, he was the Leader of the Department of Central Avionic Systems with the German Aerospace Center, Bremen. He has been involved in a vast number of projects related to aerospace systems, telecommunications, and computing systems.

He has been a Professor and the Chair of the Institute of Aerospace Information Technology with the University of Würzburg, Germany, since 2010.

• • •